# Selective Cleavage of D-Ala-D-Lac by Small Molecules: Re-Sensitizing Resistant Bacteria to Vancomycin

Gabriela Chiosis[1]*† and Ivo G. Boneca[2]‡

**Pathogenic enterococci are becoming resistant to currently available antibiotics, including vancomycin, the drug of last resort for Gram-positive infections. Enterococci pose a significant public health threat, not least because of the risk of transferring vancomycin resistance to the ubiquitous *Staphylococcus aureus*. Vancomycin resistance is manifested by cell wall peptidoglycan precursors with altered termini that cannot bind the antibiotic. Small molecules with well-oriented nucleophile-electrophile assembly and complementary chirality to the peptidoglycan termini were identified as catalytic and selective cleavers of the peptidoglycan precursor depsipeptide. These molecules were tested in combination with vancomycin and were found to re-sensitize vancomycin-resistant bacteria to the antibiotic.**

The first antibiotic-resistant strain of *Staphylococcus aureus* was identified even before the commercialization of penicillin (*1*). Over the past decade, the incidence of staphylococcal strains resistant to virtually all antibiotics has increased, although they mostly remain sensitive to vancomycin (*2*). This antibiotic is considered to be the last resort for the treatment of infections caused by Gram-positive bacteria. Unfortunately, enterococci are becoming increasingly resistant to vancomycin, raising fears that the high-level resistance genes will be transferred to staphylococci (*3*–*5*). Like the family of β-lactam antibiotics, vancomycin acts on cell wall metabolism. By binding to the D-Ala-D-Ala moiety of bacterial peptidoglycan precursors, vancomycin interferes with the growth of the cell wall (*6*). In vancomycin-resistant enterococci (VRE) bearing the *vanA* or *vanB* gene cluster, some of the D-Ala-D-Ala termini of the peptidoglycan precursors are substituted by D-Ala-D-Lac (*7*–*10*). As a result, vancomycin's affinity for the peptidoglycan layer is diminished by a factor of over 1000 (*10*). Levels of resistance are directly proportional to the percentage of precursors carrying D-Ala-D-Lac (*11*).

Strategies to bypass resistance have involved modifying vancomycin to enhance its binding to D-Ala-D-Lac and seeking inhibitors of the D-Ala-D-Lac biosynthetic pathway (*12*–*14*). Another approach involves the selective and catalytic cleavage of the D-Ala-D-Lac depsipeptide by small molecules. We hypothesized that reducing the concentration of precursors with altered termini should re-sensitize resistant bacteria to vancomycin. Such a molecule could be used in concert with vancomycin (or vancomycin derivatives with a higher affinity for peptidoglycan precursors) for the treatment of *vanA*- or *vanB*-resistant strains.

To identify small molecules that cleave the altered cell wall peptidoglycan precursors, we prepared a red dye–labeled D-Ala-D-Lac probe (Fig. 1A, **1**). Screening of nonbiased combinatorial libraries (*15*) against the labeled depsipeptide revealed that in every library the active beads carried serine at the amino-terminal position (*16*). No other nucleophiles, including Thr, Lys, or terminal amino functionalities, had this activity (*17*). A 50,000-member acylated tripeptide library yielded only three active sequences: X-L-Lys-L-Ser dimethylurea (where X is variable), X-D-Lys-D-Ser dimethylurea, and L-Lys-D-Pro-L-Ser dimethylurea (*18*). The exclusive presence of dimethylurea (the best electron donor of the series) is remarkable because 14 other acylating groups were present in the library. It appears all active sequences carry a nucleophile (amino-terminal Ser) and an electrophile (Lys, $Cu^{2+}$, NH). These must be oriented to allow for the nucleophilic attack of serine. Additionally, the nucleophilicity of the hydroxyl group of serine must be enhanced (i.e., by an internal hydrogen bond with the dimethylurea group). The prevalence of Pro in the active molecules suggests that this amino acid may be involved in inducing conformational rigidity and, therefore, pre-organization of the active sites. Molecular modeling studies were performed on the sequence BnNH-L-Lys-D-Pro-L-Ser dimethylurea (peptide **4a**, Fig. 1C) in complex with D-Ala-D-Lac (*19*) to support the structural observations deduced from the combinatorial assays (Fig. 2A).

Peptide **4a** was synthesized, and its effectiveness in cleaving D-Ala-D-Lac in physiologically relevant conditions was found to be modest: only 20% of the depsipeptide was cleaved within 24 hours (*20*). However, when the control sequences **6**, **7**, **8** (Fig. 1C) were used alone or when **6** and **8** were used in combination (*21*), the rate of hydrolysis was not significantly altered compared with buffer. This indicates that the whole structural assembly is necessary for the reaction to occur. The enantiomer of **4a** (peptide D-Lys-L-Pro-D-Ser dimethylurea that was never found as an active sequence in the combinatorial library assays) was less than half as active. This suggests that chiral complementarity is required between the depsipeptide and the cleaving molecule and that a complex is formed between the two molecules before the cleavage of the D-Ala-D-Lac ester bond.

The peptides identified from the screening of the nonbiased combinatorial libraries were not useful therapeutic agents, owing to their low catalytic activity and their ability to be easily assimilated by the bacteria and used as nutrients. The goal of these screens was to elucidate the key elements required for selective and catalytic cleavage of the altered peptidoglycan termini and to assemble these attributes in a simple structure with catalytic properties. N-acylated prolinol derivatives (Fig. 1D) are the simplest structures that fulfill these requirements. Prolinols are attractive candidates because their primary alcohol functional group forms an internal H-bond with the amide, generating an enhanced nucleophile. Furthermore, the molecules permit the addition of an electrophilic group ($NH_2$) through various linkers. Last but not least, prolinols are intrinsically chiral molecules. We designed the SProC5 molecule, which was twice as active as peptide **4a**, cleaving 50% of the depsipeptide in 24 hours (Fig. 2C). The higher activity of SProC5 compared with **4a** can be attributed to the enhanced nucleophilic nature of its hydroxyl group [H position in $^1H$ nuclear magnetic resonance (NMR), 7.59 parts per million (ppm) versus 6.62 ppm, respectively]. Molecular modeling of the SProC5 and D-Ala-D-Lac complex confirmed the structural fit of this small molecule for the cleavage of the depsipeptide (Fig. 2B).

We tested the activity of the N-acety-

[1]Department of Chemistry, Columbia University, New York, NY 10027, USA. [2]Laboratory of Microbiology, The Rockefeller University, New York, NY 10021, USA.

*To whom correspondence should be addressed. E-mail: chiosisg@mskmail.mskcc.org. Inquiries regarding the biological assays should be addressed to I. G. Boneca. E-mail: bonecai@pasteur.fr

†Present address: Memorial Sloan-Kettering Cancer Center, Department of Medicine, New York, NY 10021, USA.

‡Present address: Institut Pasteur, Unite de Pathogenie Bacterienne des Muqueuses, 75724 Paris Cedex 15, France.

lated prolinol derivatives (*22*) against the high-level vancomycin-resistant *Enterococcus faecium* strain EF228 (*23*), which is *vanA* positive and has a minimum inhibitory concentration (MIC) to vancomycin of 500 μg/ml (Fig. 3). SProC5 (50 mM) combined with vancomycin reduced the MIC to 62.5 μg/ml, i.e., an eightfold decrease (Fig. 3A). Bactericidal activity was confirmed by determining the number of cells that survived the combination of vancomycin and SProC5 (Fig. 3A, bars). Indeed, 62.5 μg/ml vancomycin plus 50 mM SProC5 resulted in a three-log decrease in bacterial load compared with vancomycin (250 μg/ml) or SProC5 (50 mM) alone. A four-log decrease in bacterial load was observed when 250 μg/ml of vancomycin was used with 50 mM SProC5. The synergistic effect of SProC5 was dose-dependent (Fig. 3B). Alone, SProC5 had no inhibitory or bactericidal activity against strain EF228.

Synergy with vancomycin could be a distinct mechanism from the mechanism predicted by the specific hydrolytic activity of SProC5. To determine whether this is the case, we compared SProC5 activity to the related molecule SProC2, which had a lower D-Ala-D-Lac hydrolytic activity in our kinetic assays (see Fig. 2C). As predicted from its hydrolytic activity, SProC2 (50 mM) showed less synergy with vancomycin and had a MIC decreased only by a factor of 2 (see Fig. 3B).

SProC5 activity was compared with that of its enantiomer, RProC5, and with its corresponding five-carbon unit (C5). None of the control molecules showed any synergy with vancomycin, even at 100 mM (see Fig. 3C), suggesting that the basis for the biological activity of SProC5 is indeed derived from its enhanced and specific D-Ala-D-Lac hydrolytic activity.

Lastly, we tested the N-acetylated prolinol derivatives against the well-characterized vancomycin-sensitive *Enterococcus faecalis* strain JH2-2 (*24*), which only synthesizes peptidoglycan precursors with D-Ala-D-Ala termini. The sensitivity of JH2-2 to vancomycin was unaffected by the synthetic molecules (Fig. 3D), showing that their biological activities are selective for strains carrying altered peptidoglycan precursors.

Random screening of almost 300,000 peptidic compounds for their ability to cleave the termini of bacteria peptidoglycan precursors bearing D-Ala-D-Lac identified active sequences with surprising similarity. Consequently, a simple small molecule, SProC5, was designed to bear structural features that cleaved the depsipeptide and increased the sensitivity of VRE to vancomycin. Our results suggest that SProC5 enhanced vancomycin activity because of its D-Ala-D-Lac hydrolytic activity.

Thus, molecules that catalytically and selectively cleave the altered termini of cell wall peptidoglycan precursors can disable the antibiotic-resistance mechanism of Gram-positive bacterial pathogens. Even SProC5, a molecule with modest in vitro catalytical activity, but with good selectivity, could resensitize VRE to vancomycin. Thus, restoration of vancomycin activity with small molecules that cleave the altered peptidoglycan components is a promising strategy.

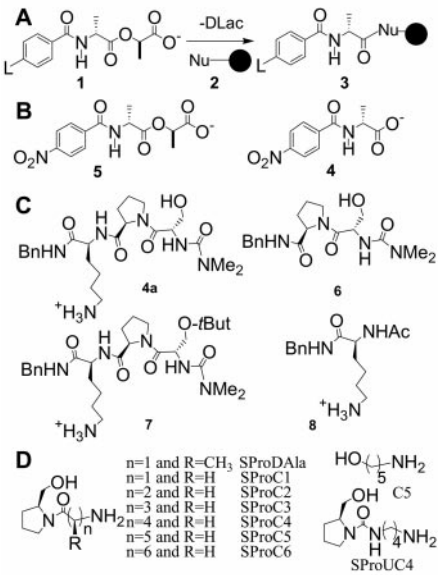


**Fig. 1.** (**A**) Approach for identifying sequences capable of cleaving the D-Ala-D-Lac depsipeptide. A library of nucleophiles (**2**) was equilibrated with a red-labeled D-Ala-D-Lac (**1**). Active nucleophiles formed a transesterification intermediate (**3**) that was not hydrolyzed in the organic media used for the assay and remained covalently linked to the solid support. Thus, beads capable of cleaving the ester bond of the depsipeptide became red (**3**) and could be selected from the mixture of inactive beads (white, **2**). We assumed that any noncovalently bound material could be washed away with a polar solvent (*15*). L, Disperse Red 1 dye; solid circle, bead. (**B**) Structure of the *p*-nitrobenzoic acid labeled D-Ala-D-Lac (**5**) and of the hydrolytic cleavage product (**4**). The two derivatives were used to determine the hydrolytic activity of the small molecules in aqueous conditions (unlike the Disperse Red 1 analog **1**, derivatives **4** and **5** are water soluble). The *p*-nitrobenzoyl label allowed monitoring the compounds under UV light due to its strong absorbance at 275 nm. (**C**) Schematic representation of the peptidic sequences (**4a**, **6**, **7**, **8**) and (**D**) the designed prolinol-based small molecules that were assayed for their ability to cleave the depsipeptide.

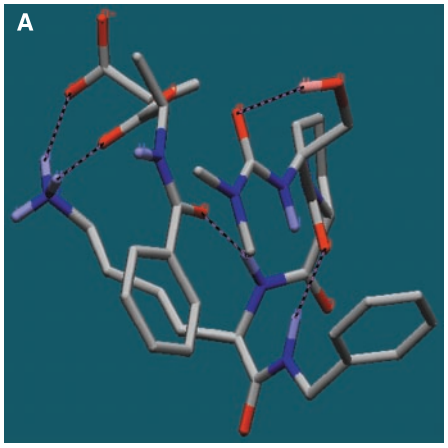


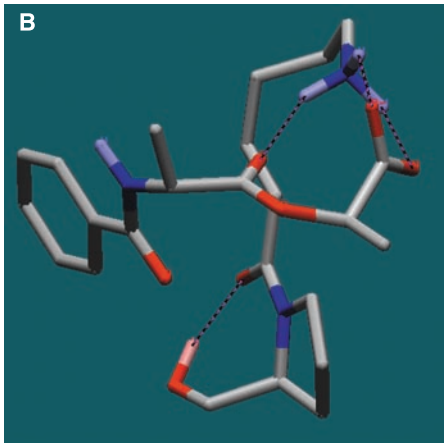


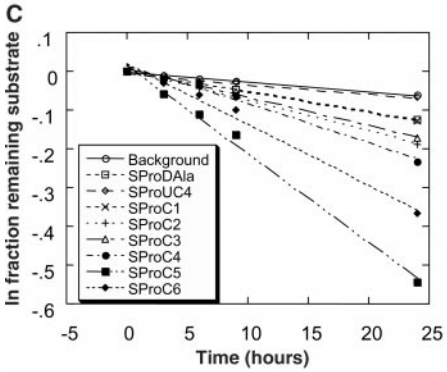


**Fig. 2.** (**A**) Computer-generated model of the **4a** complex with PhNH-D-Ala-D-Lac. The structural skeleton permits Lys and Ser to be in close proximity. Lys binds the carboxylate group of D-Ala-D-Lac and is the electrophilic amino acid that stabilizes the tetrahedral transition state. The nucleophilicity of Ser is enhanced by hydrogen bonding to the urea-capping group, and its hydroxyl is favorably positioned for attacking the depsipeptide ester group. (**B**) Structure of the complex of PhNH-D-Ala-D-Lac with SProC5 as determined by molecular modeling. Calculated hydrogen bonds are depicted by dashed lines. (**C**) Representative kinetic data for the hydrolysis of **5** (Fig. 1B) by 20 mM phosphate buffer pH 7.0, SProDAla, SProUC4, SProC1, SProC2, SProC3, SProC4, SProC5, SProC6. Substrate **5** was used at 0.5 mM, and the prolinol derivatives were used at 12 mM (*20*). The graph shows the average data from three independent experiments. Activity declined in the series as the chain length decreased from five carbons to one. A six-carbon chain was also less active (*27*).

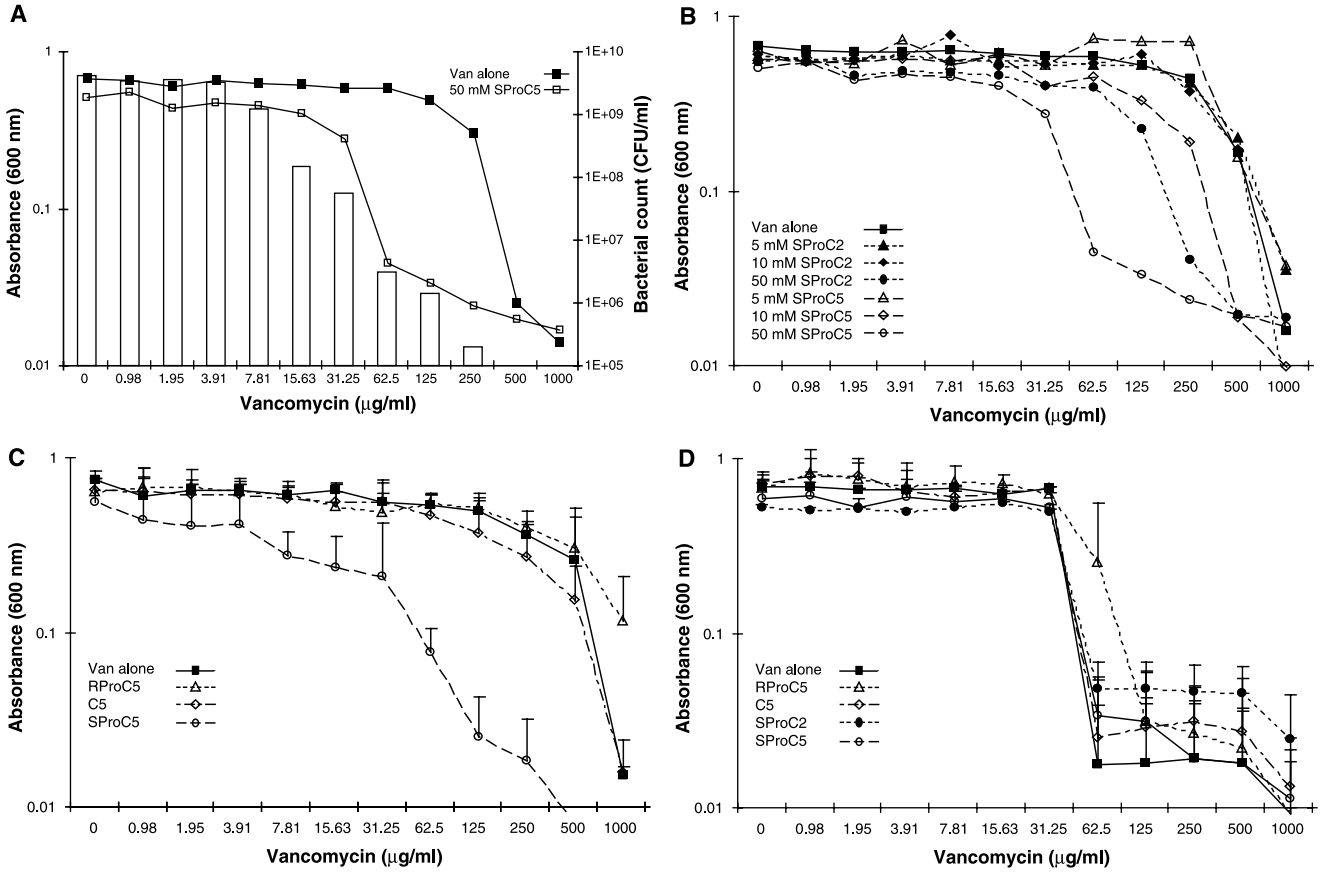


**Fig. 3.** (**A**) Strain EF228 was grown in the presence of increasing concentrations of vancomycin with or without the small molecule SProC5 (50 mM). Bactericidal activity was estimated by determining the number of CFU/ml that survived the combination of vancomycin and SProC5 (bars). (**B**) Two structurally related molecules, SProC2 and SProC5, were compared for their relative synergy with vancomycin. Their activities were concentration-dependent (0, 5, 10, and 50 mM), and SProC5 was found to be the most efficient molecule, mirroring the kinetic assays (see Fig. 2C). (**C**) The specificity of SProC5 and vancomycin against strain EF228 was tested by comparing to its enantiomer, RProC5, and its five-carbon unit, C5. Results represent the average of four independent experiments at the fixed concentration of 100 mM. (**D**) Strain JH2-2 was used as a representative vancomycin-sensitive strain that does not synthesize altered D-Ala-D-Lac terminating peptidoglycan precursors. The sensitivity of JH2-2 to vancomycin was unaffected by the addition of the synthetic molecules. Results represent the average of two independent experiments.


**References and Notes**

1. E. P. Abraham, E Chain, *Nature* **146**, 837 (1940).
2. F. C. Tenover, J. W. Biddle, M. V. Lancaster, *Emerg. Infect. Dis.* **7**, 327 (2001).
3. N. Woodford, *J. Med. Microbiol.* **47**, 849 (1998).
4. T. M. Perl, *Am. J. Med.* **106** (no. 5A), 26S (1999).
5. G. L. French, *Clin. Infect. Dis. Suppl.* **1**, S75 (1998).
6. P. E. Reynolds, *Eur. J. Microbiol. Infect. Dis.* **8**, 943 (1989).
7. G. D. Wright, C. T. Walsh, *Acc. Chem. Res.* **25**, 468 (1992).
8. C. T. Walsh, *Science* **261**, 308 (1993).
9. B. L. M. De Jonge, S. Handwerger, D. Gage, *Microb. Drug Resist.* **2**, 225 (1996).
10. T. D. Bugg *et al., Biochemistry* **30**, 10408 (1991).
11. M. Arthur, F. Depardieu, P. Reynolds, P. Courvalin, *Mol. Microbiol.* **21**, 33 (1996).
12. R. Xu, G. Greiveldinger, L. E. Marenus, *J. Am. Chem. Soc.* **121,** 4898 (1999).
13. M. Ge *et al., Science* **284**, 507 (1999).
14. U. N. Sundram, J. H. Griffin, T. I. Nicas, *J. Am. Chem. Soc.* **118**, 13107 (1996).
15. To the library beads, we added 200 μl of substrate **1** (2.3 mM) in 1,2-dichloroethane or dimethylformamide (DMF), and the mixture was rotated for 3 to 5 days in a small glass vial. DMF was added and shaking continued for 1 hour. The solvent was removed and the DMF wash was repeated several times. One wash was performed with one drop of benzylamine added to DMF to remove any remaining physically bound substrate. The strongly red beads were selected individually and added to 1.5-μl DMF (in 25-μl capillary tubes) and photolysed for 6 hours under a short wave UV lamp. Decoding was achieved by injecting the content of each capillary into an electron capture–gas chromatograph (EC-GC) and comparing the chromatogram to a standard (*25*, *26*).
16. For a detailed description of the libraries used for screening, the resulting active sequences, screening methodology, and the synthesis and characterization of all described compounds, see supplementary materials (*21*).
17. All peptides were side chain deprotected and washed with dichloromethane (DCM)-triethylamine after trifluoroacetic acid (TFA) deprotection to ensure that all possible nucleophiles were in the unprotonated state.
18. Selectivity for library SSY was improved by using DMF as the assay solvent and by reducing the concentration of the substrate to 0.85 mM (the lower threshold for visual detection of red beads).
19. Simulations were performed using the General Born/Surface Area solvation method for water and AMBER* force field, as implemented in Macromodel version 6.0. We used Monte Carlo multiple minimum (MCMM) alternated with low-frequency mode conformational search (LMCS) as conformational search methods. MCMM was better at finding minima different from the initial conformations, whereas LMCS was better at finding minima close to the initial conformations. Generally, a search was started with MCMM, the output conformations were re-minimized, and the conformations lower than 3 or 5 kcal were used as input for a new search using LMCS until convergence was obtained.
20. Stock solutions of 16 mM of **5** (Fig. 1B) and 130 mM of peptide or small molecules (Fig. 1, C and D) were made in water. Phosphate buffer solution of 25 mM was made by adjusting the pH of a $K_2HPO_4$ solution to 7.0 by the addition of concentrated HCl. We added to a 1.5-ml glass vial (Waters) a 5-μl stock solution of **5** and 15-μl stock solution of peptide, followed by 135 μl of buffer. The volume was adjusted to 160 μl with water. Vials were incubated at 37°C and 2-μl aliquots were taken every 3 hours. Each aliquot was diluted with water to 5 μl, and 2 μl were used for high-performance liquid chromatography (HPLC). Separation of components was carried out on a reverse phase column C18 (Waters, Milford Lakes, MA) using a water-acetonitrile (0.1% TFA) gradient. We used HPLC and monitored the *p*-$NO_2$-phenyl derivative by ultraviolet (UV) at 275 nm, to follow the disappearance of derivative **5** and the formation of the hydrolyzed product **4** (see Fig. 1B).
21. Web figures 1 through 10, Web scheme 1, Web tables 1 through 6, and supplemental text are available at *Science* Online at www.sciencemag.org/cgi/content/full/293/5534/1484/DC1.
22. *Enterococcus faecium* EF228 (*23*), a *vanA* strain, and *E. faecalis* strain JH2-2 (*24*) were grown on BHI (Difco or Oxoid) agar or broth at 37°C. Biological assays were performed in 96-well tissue culture plates (MICROTEST U-bottom, Falcon, Becton Dickinson, Franklin, NJ). A range of vancomycin (Sigma) concentrations (100 μl per well) were used based on sequential twofold dilution starting from 100 and 2000 μg/ml to 0.1 and 1.96 μg/ml for

strains JH2-2 and EF228, respectively. The different molecules were added (100 μl per well) at fixed concentrations (0, 5, 10, 50, and 100 mM) containing an inoculum of either strain at a final dilution of $10^{-2}$ obtained from an overnight culture. The range of effective vancomycin concentrations started at 50 and 1000 μg/ml for JH2-2 and EF228, respectively. Micro-titer plates were incubated at 37°C without agitation for 18 hours. Cell sediments were resuspended by shaking, and optical density (OD) of 600 nm was measured with an ELISA (enzyme-linked immunosorbent assay) Multiskan RC plate reader (Labsystems, Helsinki, Finland). Bactericidal activity was determined by serially diluting ($10^{-2}$, $10^{-4}$, and $10^{-5}$) each well in BHI broth and by plating 10 μl of each dilution on BHI agar plates. Plates were incubated for 24 hours and the number of colony-forming units per milliliter (CFU/ml) was determined.

23. S. Handwerger, M. J. Pucci, A. Kolokathis, *Antimicrob. Agents. Chemother.* **34**, 358 (1990).
24. A. E. Jacob, S. J. Hobbs, *J. Bacteriol.* **117**, 360 (1974).
25. M. H. J. Ohlmeyer *et al.*, *Proc. Natl. Acad. Sci. U.S.A.* **90**, 10922 (1993).
26. H. P. Nestler, P. A. Bartlett, W. C. Still, *J. Org. Chem.* **59**, 4723 (1994).
27. For a detailed study, see supplemental materials (*21*).
28. We thank W. Clark Still and A. Tomasz for providing materials and intellectual support and for critically reviewing this manuscript and C. Watson and J. Rothman for assistance and for helpful discussions. We are grateful for critical review of this manuscript by A. Labigne, H. de Reuse, C. Le-Bouguenec, T. Muir, N. Rosen, and S. Shuman. Supported by NIH. I.G.B. was supported by a fellowship from the Praxis XXI program (BD/2379/94, Portugal).

1 March 2001; accepted 3 July 2001

# Enhanced Neurofibrillary Degeneration in Transgenic Mice Expressing Mutant Tau and APP

**Jada Lewis,* Dennis W. Dickson,* Wen-Lang Lin, Louise Chisholm, Anthony Corral, Graham Jones, Shu-Hui Yen, Naruhiko Sahara, Lisa Skipper, Debra Yager, Chris Eckman, John Hardy, Mike Hutton,† Eileen McGowan**

**JNPL3 transgenic mice expressing a mutant tau protein, which develop neurofibrillary tangles and progressive motor disturbance, were crossed with Tg2576 transgenic mice expressing mutant β-amyloid precursor protein (APP), thus modulating the APP-Aβ (β-amyloid peptide) environment. The resulting double mutant (tau/APP) progeny and the Tg2576 parental strain developed Aβ deposits at the same age; however, relative to JNPL3 mice, the double mutants exhibited neurofibrillary tangle pathology that was substantially enhanced in the limbic system and olfactory cortex. These results indicate that either APP or Aβ influences the formation of neurofibrillary tangles. The interaction between Aβ and tau pathologies in these mice supports the hypothesis that a similar interaction occurs in Alzheimer's disease.**

Alzheimer's disease (AD) is pathologically characterized by senile plaques, largely composed of extracellular deposits of Aβ peptide, and neurofibrillary tangles (NFTs), composed of intracellular filamentous aggregates of hyperphosphorylated tau protein. Since the initial molecular characterizations of these lesions (*1–3*), there has been controversy over how these lesions and their constituent molecules are pathogenically related to each other and to the neuronal and synaptic losses that characterize the disease (*4–6*). A key part of this debate has been the observation that the pathogenic mutations that underlie the autosomal dominant forms of the disease—mutations in APP or in the presenilins PS-1 and PS-2 (*7–9*)—lead to increased production of the Aβ42 peptide in tissues from affected individuals (*10*), in transfected cells (*11–13*), and in transgenic animals (*12, 14–18*). Some transgenic mouse models for AD, overexpressing mutant human APP alone or with mutant PS-1, develop senile plaques; however, these mice lack NFTs and exhibit little neuronal loss (*14–18*). This has limited their use as models of disease and fueled the notion that senile plaques and NFTs are generated by independent processes.

Neurofibrillary pathology is also a feature of other neurodegenerative diseases, including FTDP-17 (frontotemporal dementia and Parkinsonism linked to chromosome 17). Mutations in the *tau* gene underlie FTDP-17, hence tau dysfunction is sufficient to cause neurodegeneration (*19*). Furthermore, JNPL3 transgenic mice with the $Pro^{301} \rightarrow Leu$ (P301L) tau mutation develop NFTs in the basal telencephalon, diencephalon, brainstem, and spinal cord, along with neuronal loss that is most evident in the spinal cord, especially in the anterior horn (*20*).

The production of these mutant tau transgenic mice provided the opportunity to test experimentally whether the distribution or timing of neurofibrillary pathology is influenced by the pathogenic mutations that cause AD. Therefore, we crossed Tg2576 transgenic mice expressing the APPsw mutation ($Lys^{670} \rightarrow Asn$, $Met^{671} \rightarrow Leu$) (*15, 21, 22*) with JNPL3 transgenic mice expressing mutant P301L four-repeat tau (*20*) and compared the pathology of the crossed mice with each of their parental lines (*23*).

Previous studies have shown that Tg2576 mice have markedly elevated Aβ levels at an early age and develop extracellular Aβ deposits in the cortex and hippocampus by 9 to 12 months of age (*15*). Hemizygous JNPL3 mice develop progressive motor and behavioral abnormalities with robust neurofibrillary pathology and neuronal loss in the spinal cord as early as 6.5 months (*20*). In JNPL3 animals, NFTs are primarily located in the spinal cord and the hindbrain, with fewer NFTs in the midbrain, amygdala, and hypothalamus (*20*). Pretangles, which are neurons that have abnormal expression of phospho-tau epitopes, are found in greater numbers and have a wider distribution throughout the spinal cord and brain, most notably in limbic structures such as the hippocampus and amygdala. Neither pretangles nor NFTs are detected in the basal ganglia of JNPL3 mice.

We examined the brains and spinal cords of Tg2576 × JNPL3 progeny at 2.5 to 3.5 months, 6 to 7 months, and 8.5 to 15 months of age (*24–29*). These progeny included double mutant tau (P301L)–mutant APP (APPsw) (hereafter termed TAPP mice), mutant tau (JNPL3), mutant APP (Tg2576), and nontransgenic animals. TAPP mice had amyloid plaques similar in number and distribution to those of comparably aged Tg2576 mice. Plaques were detected as early as 6 months of age but became numerous only in older TAPP and Tg2576 mice (8.5 to 15 months) in the olfactory cortex, cingulate gyrus, amygdala, entorhinal cortex, and hippocampus (Fig. 1) (*30*). NFTs were morphologically similar in TAPP and JNPL3 mice and appeared in the spinal cord and pons as early as 3 months of age, but were consistently present and numerous only in older animals (Figs. 2 and 3). Some of the NFTs were fluorescent when stained with thioflavin-S, and all were intensely positive for Gallyas silver stain and immunoreactive with a panel of antibodies to tau protein, including antibodies to phosphorylation-dependent and conformational epitopes (*24–28*) (Fig. 1). Ultrastructurally, NFTs in the TAPP mice were also similar to those in JNPL3 mice and were composed of straight filaments, 17 to 22 nm

Birdsall Building, Mayo Clinic Jacksonville, 4500 San Pablo Road, Jacksonville, FL 32224, USA.

*These authors contributed equally to this report.
†To whom correspondence should be addressed. E-mail: hutton.michael@mayo.edu